RNA15 can bind to poly(U) ribopolymers (*20*), which suggests that the generally U-rich RNA sequences important for 3′ processing in yeast (*4*, *21*) may be recognized by this protein. The finding that this putative RNA-binding protein is a component of CF I may thus help to elucidate the sequence requirements in yeast 3′-end processing. It is worth noting in this context that the mammalian counterpart of yeast CF I, cleavage and polyadenylation specificity factor (CPSF), is a sequence-specific RNA-binding factor consisting of multiple polypeptides (*1*, *22*).

REFERENCES AND NOTES

1. E. Wahle and W. Keller, *Annu. Rev. Biochem.* **61**, 419 (1992).
2. J. S. Butler and T. Platt, *Science* **242**, 1270 (1988); D. Patel and J. S. Butler, *Mol. Cell. Biol.* **12**, 3297 (1992); J. S. Butler, P. P. Sadhale, T. Platt, *ibid.* **10**, 2599 (1990).
3. C. L. Moore and P. A. Sharp, *Cell* **36**, 581 (1984).
4. J. Chen and C. Moore, *Mol. Cell. Biol.* **12**, 3470 (1992).
5. J. Lingner, I. Radtke, E. Wahle, W. Keller, *J. Biol. Chem.* **266**, 8741 (1991); J. Lingner, J. Kellermann, W. Keller, *Nature* **354**, 496 (1991).
6. J. C. Bloch, F. Perrin, F. Lacroute, *Mol. Gen. Genet.* **165**, 123 (1978); L. Minvielle-Sebastia, B. Winsor, N. Bonneaud, F. Lacroute, *Mol. Cell. Biol.* **11**, 3075 (1991).
7. L. Guarente, *Trends Genet.* **9**, 362 (1993); T. Huffaker, M. Hoyt, D. Botstein, *Annu. Rev. Genet.* **21**, 259 (1987); D. Frank, B. Patterson, C. Guthrie, *Mol. Cell. Biol.* **12**, 5197 (1992); X. C. Liao, J. Tang, M. Rosbash, *Genes Dev.* **7**, 419 (1993).
8. The relevant genotypes of the starting strains are as follows: LM61 (*rna14-1*, *pap1Δ::LEU2*, *ura3-1*, *trp1-1*, *ade2-1*, and p*PAP1*) and LM62 (*rna15-1*, *pap1Δ::LEU2*, *ura3-1*, *trp1-1*, *ade2-1*, and p*PAP1*). p*RNA14* and p*RNA15* are *TRP1*-marked low-copy plasmids containing genomic fragments allowing complementation of *rna14* and *rna15* mutations, respectively. pA*pap1-5* is a low-copy *ADE2*-marked plasmid carrying the *pap1-5* mutant allele (*9*, *23*).
9. P. J. Preker and W. Keller, unpublished results. Eight different temperature-sensitive mutant alleles, called *pap1-2* to *pap1-9*, were generated by polymerase chain reaction mutagenesis with the use of either low deoxyadenosine triphosphate (dATP) concentration or inclusion of manganese in the reaction. These mutants were sequenced, and most of them showed multiple mutations. In vitro, the extract of the *pap1-5* mutant used in this study shows approximately 50% of specific polyadenylation activity as compared with that of a wild-type extract.
10. J. D. Boeke, F. Lacroute, G. R. Fink, *Mol. Gen. Genet.* **197**, 345 (1984).
11. The extracts were made as described elsewhere (*2*), except that cells were grown at 24°C and converted to spheroplasts with the use of Zymolyase-100T (Seikagaku Kogyo, Tokyo) at a concentration of 300 μg/ml. The names and genotypes of the strains are as follows: LM88 (*rna14-1*; *ura3-1*; *trp1-1*; *ade2-1*; *leu2-3,112*), LM91 (*rna15-1*; *ura3-1*; *trp1-1*; *ade2-1*; *leu2-3,112*), and LM98 (*ura3-1*; *trp1-1*; *ade2-1*; *leu2-3,112*; *his3-11,15*; *pap1Δ::LEU2*; and pA*pap1-5*). They are isogenic with strain W303 (*ura3-1*; *trp1-1*; *ade2-1*; *leu2-3,112*; *his3-11,15*, from R. Rothstein, Columbia University, New York), which was used to prepare the wild-type extract. The pA*pap1-5* plasmid contains the *pap1-5* mutant allele (*9*) cloned into an *ADE2*-marked low-copy vector (pASZ11) (*23*).
12. A standard in vitro processing reaction was done in a 25-μl reaction volume containing 2 μl of extract, 1.6 mM Hepes-KOH (pH 7.9), 0.016 mM EDTA, 4 mM potassium chloride, 1.04 mM dithiothreitol, 1.6% glycerol, 2% polyethylene glycol, 75 mM potassium acetate, 1.8 mM magnesium acetate, 2 mM ATP, 20 mM creatine phosphate, creatine kinase (0.2 mg/ml), 0.01% NP-40, and ~0.2 units of RNAguard (Pharmacia). When only the cleavage reaction was assayed, CTP replaced ATP, and EDTA was used instead of magnesium acetate, which prevents poly(A) addition and degradation of the 3′ fragment (*4*). The reactions were incubated at the temperatures and for the times indicated in the figure legends. They were stopped by addition of 75 μl of a stop solution [100 mM tris-HCl (pH 8), 150 mM NaCl, 12.5 mM EDTA, 1% SDS, proteinase K (0.2 mg/ml), and glycogen (0.05 mg/ml)] and incubated for 1 hour at 42°C. The RNAs were recovered by precipitation and analyzed as described (*4*). For complementation assays, the extracts were mixed in a 1:1 ratio.
13. S. W. Ruby, T. H. Chang, J. Abelson, *Genes Dev.* **7**, 1909 (1993).
14. L. Minvielle-Sebastia, unpublished results.
15. The synthesis of the short tracts observed with *rna14* and *rna15* mutant extracts still depends on the $(UA)_6$ cis-acting sequences of the *GAL7* precursor, because no polyadenylation was obtained with the mutant precleaved RNA (*GAL7-7*), in which these signals were deleted (*4*).
16. N. Bonneaud, L. Minvielle-Sebastia, C. Cullin, F. Lacroute, *J. Cell Sci.* **107**, 913 (1994).
17. Fifty microliters of crude anti-serum or preimmune serum directed against RNA14p, RNA15p, or PAP1 was coupled to ≈40 μl of packed protein A–Sepharose (PAS) preequilibrated with buffer E (*4*) plus 0.01% NP-40 for 3 hours at 4°C. After three washes with the same buffer, 70 μl of a wild-type extract was added to the resin and incubated for 4 hours at 4°C on a wheel. The supernatant was reapplied on a fresh antibody-PAS resin for a second round of depletion. The wild-type strain used here and for the fractionation of the 3′-processing factors is a commercial brewery *S. cerevisiae* strain, referred to as VDH2 (Versuchanstalt der Hefeindustrie, Berlin, Germany). The cells were broken in a Bead Beater (BioSpec, Bartlesville, OK), and the protein extract was further prepared as previously described (*4*). Extracts made from this strain were active for 3′ processing of *CYC1*, *GAL7*, and their corresponding precleaved RNAs (*14*).
18. J. Lingner and W. Keller, unpublished results. The serum was obtained from a rabbit immunized with recombinant PAP (*5*).
19. An identical pattern of complementation was also found with the *rna15* extract. In the same way, CF I fraction 40 restored 3′-end processing activity of the extracts depleted by antibodies to RNA14 and RNA15 (*14*).
20. L. Minvielle-Sebastia, thesis, Paris University (1992).
21. K. S. Zaret and F. Sherman, *Cell* **28**, 563 (1982); P. Russo, W. Z. Li, D. M. Hampsey, K. S. Zaret, F. Sherman, *EMBO J.* **10**, 563 (1991); W. Hou, R. Russnak, T. Platt, *ibid.* **13**, 446 (1994).
22. A. Jenny, H. P. Hauri, W. Keller, *Mol. Cell. Biol.* **14**, 8183 (1994).
23. A. Stotz and P. Linder, *Gene* **95**, 91 (1990).
24. The Taq I fragment overlapping the 3′ untranslated region of the *CYC1* gene [from position 351 to position 588, M. Smith *et al.*, *Cell* **16**, 753 (1979)] was introduced into the Acc I site of pGEM4 (Promega), generating the pG4-*CYC1* plasmid. The capped 301-nucleotide *CYC1* precursor was synthesized in vitro from Eco RI–restricted pG4-*CYC1* with T7 RNA polymerase. The lengths of the 5′ and 3′ cleavage products (185 and 116 nucleotides, respectively) calculated from the position of the polyadenylation site (*2*) are in good agreement with the size of the fragments seen on the gel.
25. J. Sambrook, E. F. Fritsch, T. Maniatis, *Molecular Cloning: A Laboratory Manual* (Cold Spring Harbor Laboratory, Cold Spring Harbor, NY, ed. 2, 1989).

26. Supported by the Kantons of Basel and the Swiss National Science Foundation. We thank J. Lingner for antibodies to PAP1, C. Moore for the *GAL7* constructs, and N. Bonneaud and F. Lacroute for antibodies to RNA14 and RNA15 and discussions. L.M:-S. was supported by a European Molecular Biology Organization long-term fellowship. P.J.P. is the recipient of a predoctoral fellowship from the Boehringer-Ingelheim Fonds.

22 July 1994; accepted 4 October 1994

Correction of Lethal Intestinal Defect in a Mouse Model of Cystic Fibrosis by Human *CFTR*

Lan Zhou, Chitta R. Dey; Susan E. Wert, Michael D. DuVall, Raymond A. Frizzell, Jeffrey A. Whitsett*

Cystic fibrosis (CF) is caused by mutations in the gene encoding the cystic fibrosis transmembrane conductance regulator (*CFTR*). A potential animal model of CF, the *CFTR*$^{-/-}$ mouse, has had limited utility because most mice die from intestinal obstruction during the first month of life. Human *CFTR* (h*CFTR*) was expressed in *CFTR*$^{-/-}$ mice under the control of the rat intestinal fatty acid–binding protein gene promoter. The mice survived and showed functional correction of ileal goblet cell and crypt cell hyperplasia and cyclic adenosine monophosphate–stimulated chloride secretion. These results support the concept that transfer of the h*CFTR* gene may be a useful strategy for correcting physiologic defects in patients with CF.

Cystic fibrosis mice bearing a null mutation in the *CFTR* gene lack adenosine 3′,5′-monophosphate (cAMP)–stimulated Cl^- transport in intestinal epithelial cells, which leads to goblet cell hyperplasia, intestinal obstruction, and perforation (*1*). To correct the lethal intestinal abnormalities in a group of CF mice, we used the rat intestinal fatty acid–binding protein (FABP) gene promoter (*2*) to direct expression of the wild-type h*CFTR* complementary DNA (cDNA) to the intestinal epithelial cells of these mice (*3*). A chimeric FABP-h*CFTR* gene construct was microinjected into fertilized oocytes, producing

L. Zhou, C. R. Dey, S. E. Wert, J. A. Whitsett, Children's Hospital Medical Center, Division of Pulmonary Biology, Cincinnati, OH 45229–3039, USA.
M.-D. DuVall and R. A. Frizzell, Department of Physiology and Biophysics, University of Alabama at Birmingham, Birmingham, AL 35294–0005, USA.

*To whom correspondence should be addressed.

transgenic mice from both heterozygotic $CFTR^{+/-}$ and wild-type FVB/N mice. The FABP-h*CFTR* transgene was detected by Southern (DNA) blot analysis in founder mice and their offspring, and the integrity of the DNA was confirmed by restriction fragment analysis (*4*). The transgenic mice were bred to produce $CFTR^{-/-}$ mouse lines bearing the FABP-h*CFTR* transgene.

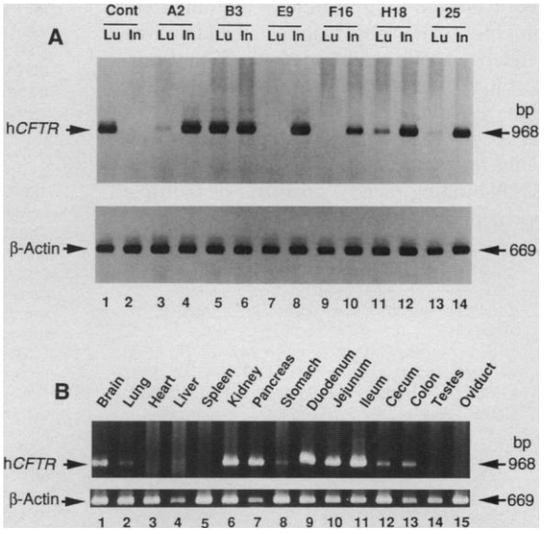

Fig. 1. The RT-PCR analysis of h*CFTR* mRNA. Reverse transcription was done on total tissue RNA with an oligo(dT) primer. Beta-actin cDNA was used as a control (cont). PCR of the h*CFTR* fragment was done with primers 5′-TAAACCTACCAAGTCAACCA-3′ and 5′-AATTCCATGAGCAAATGTC-3′. Sizes of the PCR products are shown on the right. (**A**) Expression of h*CFTR* mRNA in the intestines of transgenic mice from six transgenic lines. Lane 1 shows a positive control: lung (Lu) cDNA from the J4 transgenic mouse bearing a lung-specific SP-C–h*CFTR* construct (*10*). Lane 2 shows intestinal (In) cDNA from a transgene-negative littermate. The h*CFTR* mRNA was detected in the intestines of all six transgenic lines tested (lanes 4, 6, 8, 10, 12, and 14). It was also detected in the lungs (lanes 3, 5, 11, and 13) but was not in the lungs of lines E9 or F16 (lanes 7 and 9). (**B**) Distribution of h*CFTR* mRNA in tissues from transgenic line A2. The h*CFTR* mRNA was detected in large amounts in the duodenum, jejunum, and ileum (lanes 9 to 11), in smaller amounts in the cecum and colon (lanes 12 and 13), and in varying amounts in the brain, lung, kidney, pancreas, and stomach (lanes 1, 2, 6, 7, and 8, respectively). Gels were stained with ethidium bromide.

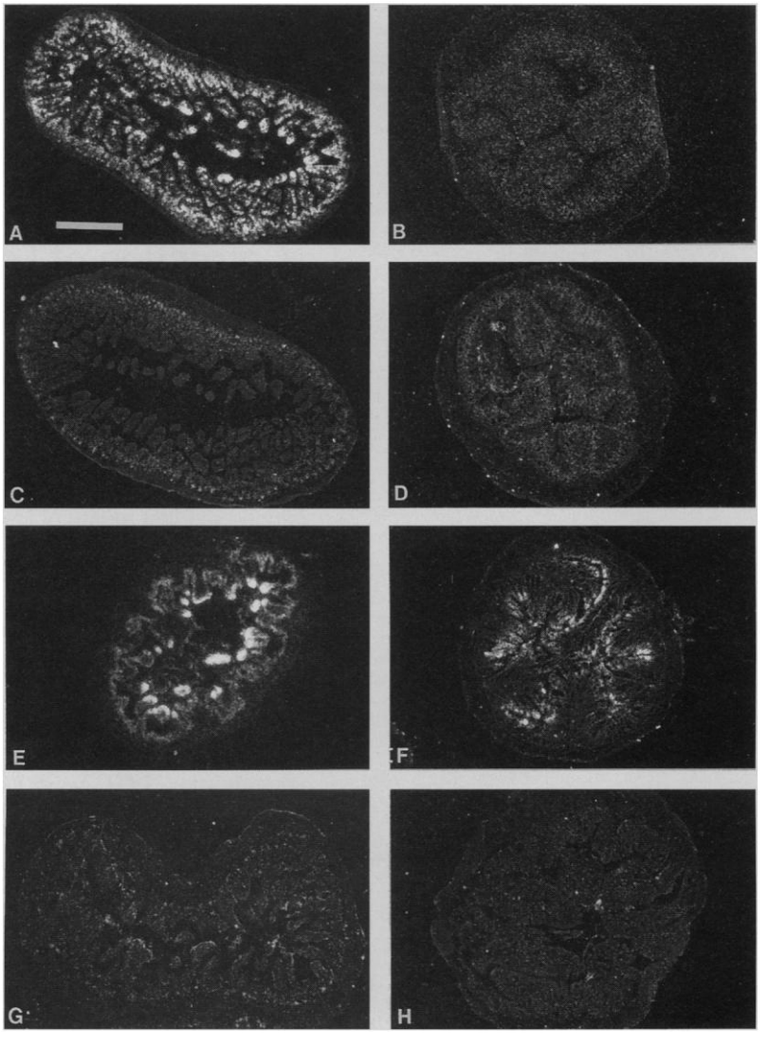

Fig. 2. In situ hybridization analysis of h*CFTR* mRNA in the adult mouse intestine. Small and large intestines from wild-type and line A2 mice were fixed in 4% paraformaldehyde. Cryostat sections (10 μm) from the ileum (**A**, **C**, **E**, and **G**) and colon (**B**, **D**, **E**, and **H**) were hybridized overnight at 42°C with [^{35}S]UTP-labeled h*CFTR* sense and antisense riboprobes (*10*). The sections were then washed stringently, treated with ribonuclease A, and exposed to Ilford K5 emulsion for 7 to 10 days at 4°C. Sections were photographed under dark-field illumination. A hybridization signal was detected by antisense riboprobe in epithelial cells of the ileum (A and E) and colon (B and F) of FABP-h$CFTR^{+/-}$ mice from both $CFTR^{+/+}$ (A and B) and $CFTR^{-/-}$ (E and F) backgrounds. No signal was detected in the ileum or colon of $CFTR^{-/-}$ mice (G and H). The h*CFTR* ribroprobe hybridized weakly with m*CFTR* mRNA in the crypt epithelial cells of the ileum and colon of $CFTR^{+/+}$ mice (C and D). Scale bar, 500 μm.

Human *CFTR* mRNA was readily detected by reverse transcription–polymerase chain reaction (RT-PCR) in the small intestine of six distinct FABP-h*CFTR* mouse lines (Fig. 1A). In several mouse lines, the h*CFTR* mRNA was expressed in the intestine and was absent or present in barely detectable amounts in the lung or nasal epithelium. In lines A2 and E9, h*CFTR* mRNA was most abundant in the ileum, jejunum, and duodenum and was less abundant in the cecum and colon (Fig. 1B). The h*CFTR* mRNA was not detected in the lungs of mice of the A2 or E9 lines by Northern (RNA) blot analysis but was detectable, albeit in small amounts, by RT-PCR in A2 but not E9 mice. Founder lines (A2, E9, and I25) were bred to $CFTR^{+/-}$ mice, which were then bred to produce homozygous $CFTR^{-/-}$ mice expressing the h*CFTR* mRNA. FABP-h$CFTR^{+/-}$–$CFTR^{-/-}$ mice from the A2 and E9 lines routinely survived weaning and showed prolonged survival (5). In contrast, 50 matings of $CFTR^{+/-}$ mice from both FVB/N and C57BL/6 backgrounds resulted in survival of less than 5% of $CFTR^{-/-}$ mice. Likewise, only 1 of 23 $CFTR^{-/-}$ mice derived from matings of FVB/N $CFTR^{+/-}$ and $CFTR^{+/-}$ mice survived.

In situ hybridization demonstrated the presence of h*CFTR* mRNA in the intestinal epithelium of FABP-h*CFTR* mice from both $CFTR^{+/+}$ and $CFTR^{-/-}$ backgrounds (Fig. 2). The h*CFTR* mRNA was most abundant in the ileum, jejunum, and duodenum and was less abundant in the colon and cecum. It was expressed in the epithelial cells of the intestinal villi but not in the crypts of Lieberkuhn. The distribution of h*CFTR* mRNA was distinct from that of the endogenous murine *CFTR* mRNA, which was present in large amounts in the colon, ileum, and jejunum in wt mice. In these tissues, *CFTR* was expressed most prominently in the crypts of Lieberkuhn, decreased in abundance in the more mature cells along the intestinal villi, and was relatively excluded from the villous tips (6). The h*CFTR* mRNA was less abundant in the colon of the transgenic mice and, in the small intestine, was excluded from crypt cells.

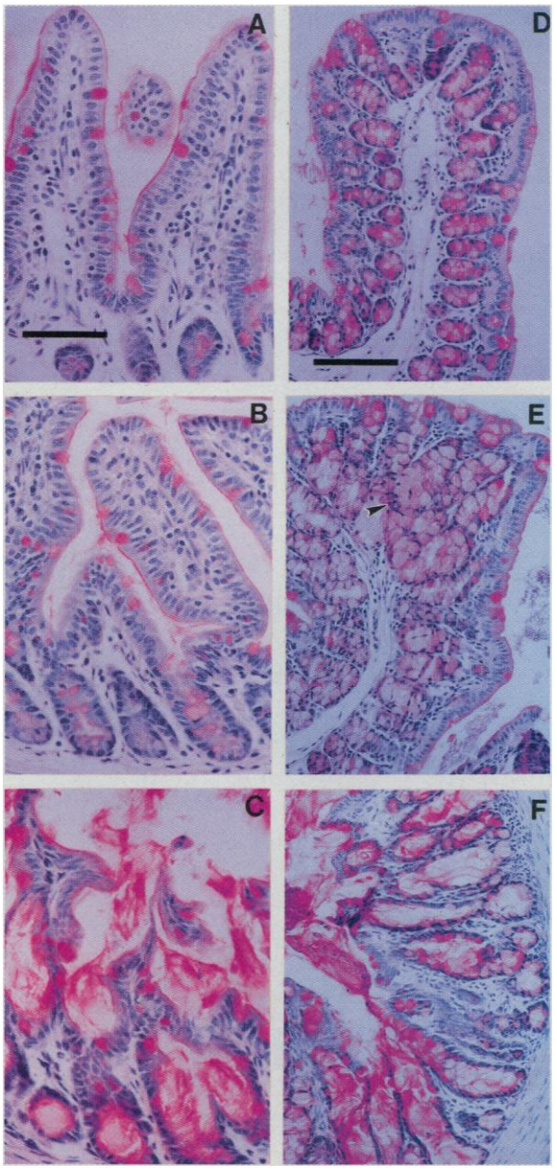

Fig. 3. PAS staining of ileal and colonic epithelium. Sections of the ileum (**A** through **C**) and colon (**D** through **F**) of $CFTR^{+/+}$ (A and D), FABP-h$CFTR^{+/-}$–$CFTR^{-/-}$ (B and E), and $CFTR^{-/-}$ (C and F) mice were stained with PAS and hematoxylin. The goblet cell hyperplasia and dilation of crypts with mucus was seen in both ileal and colonic mucosa of $CFTR^{-/-}$ mice (C and F) and was corrected in the ileal mucosa of FABP-h$CFTR^{+/-}$–$CFTR^{-/-}$ mice (B). The goblet cell hyperplasia and distension of crypt cells (arrowhead) were still seen in some areas of the colonic mucosa of FABP-h$CFTR^{+/-}$–$CFTR^{-/-}$ mice (E). Scale bar: (A through C), 64 μm; (D through F), 128 μm.

Morphologic changes in the intestinal epithelium of the wild-type (nontransgenic) and $CFTR^{-/-}$ and FABP-h$CFTR^{+/-}$–$CFTR^{-/-}$ bitransgenic mice were further assessed by periodic acid–Schiff (PAS) staining (Fig. 3). Goblet cell hyperplasia, a prominent feature of the $CFTR^{-/-}$ mice, was entirely corrected in the ileum of lines A2 and E9 FABP-h$CFTR^{+/-}$–$CFTR^{-/-}$ mice. However, the disruption of crypt epithelial cell organization and goblet cell hyperplasia seen in the colon of the $CFTR^{-/-}$ mice was not fully corrected in the FABP-h$CFTR^{+/-}$–$CFTR^{-/-}$ mice examined (three from line A2 and one from line E9), perhaps because of inadequate expression of h*CFTR* mRNA. The coiled "wormlike" cecum that was typically observed in the $CFTR^{-/-}$ mice was not observed in the FABP-h$CFTR^{+/-}$–$CFTR^{-/-}$ mice examined.

Short-circuit current (I_{sc}) measurements were made from the intestine of $CFTR^{-/-}$, bitransgenic FABP-h$CFTR^{+/-}$–$CFTR^{-/-}$, and wt mice (Fig. 4). Forskolin-induced I_{sc} (rate of cAMP-stimulated Cl^- secretion) was absent in ileal, jejunal, and colonic segments from $CFTR^{-/-}$ mice (7); phlorizin-sensitive Na^+-dependent glucose absorption was present in the jejunum and ileum. In the small intestines of the FABP-h$CFTR^{+/-}$–$CFTR^{-/-}$ mice (Fig. 4A), electrogenic Cl^- secretion was restored. Forskolin increased the I_{sc} across both jejunum and ileum of the bitransgenic animals (Fig. 4B). Addition of glucose to the mucosal solution further increased the I_{sc}, and this increase was phlorizin-sensitive. On average, these responses were greater in the ileum and jejunum of wt animals.

A forskolin-induced electrogenic Cl^- secretory response was observed in the wild-type colon but not in the colon of FABP-h$CFTR^{+/-}$–$CFTR^{-/-}$ mice. This correlated with the histopathologic changes, which persisted despite upstream expression of h*CFTR* mRNA and restoration of cAMP-stimulated Cl^- secretory activity in the small intestine. Although the amount of h*CFTR* mRNA expression in the cecum of bitransgenics was as small as that in the colon, the cecum developed normally and did not exhibit the atrophy or irregular shape that was typical of $CFTR^{-/-}$ mice. Correction of the goblet cell hyperplasia in

the ileum demonstrates the importance of *CFTR* expression and Cl^- secretion in the pathogenesis of the lethal obstructive phenotype in the small intestines of $CFTR^{-/-}$ mice. Our data suggest that the small amount of h*CFTR* mRNA in the colonic epithelium was not sufficient to fully correct the transport and histologic abnormalities in the colon of the CF mouse. In contrast, normal cecal development may depend more on luminal factors than on its *CFTR*-dependent ion transport functions.

The principal secretory activity of the small and large intestines resides in the undifferentiated cells of the crypts of Lieberkuhn (8), which correlates with the site of endogenous *CFTR* expression (6). Several features of the transport responses observed in the bitransgenic animals are consistent with expression of *CFTR* mRNA in the more differentiated villus absorptive cells. First, the forskolin-induced ΔI_{sc} was smaller than the wild-type response, which suggests that the spatially restricted expression of h*CFTR* mRNA does not quantitatively correct the Cl^- secretory response. Second, bumetanide inhibited ~60% of the forskolin-induced ΔI_{sc} in wild-type intestine but only ~30% of the ΔI_{sc} in bitransgenic animals, which suggests that the bumetanide-sensitive Na-K-2Cl cotransporter may not be the primary mechanism whereby Cl^- enters cells that express h*CFTR*. Third, glucose-stimulated I_{sc} was smaller in the bitransgenic animals. Glucose was added after forskolin, which would increase the apical Cl^- conductance, depolarize the apical membrane potential, and thereby reduce the driving force for Na-dependent glucose entry into villus absorptive cells. Thus, the features of the transport assays are consistent with a greater amount of h*CFTR* expression in villus than in crypt cells. Nevertheless, h*CFTR* mRNA and the Cl^- secretion rate that it supports are apparently sufficient to prevent intestinal obstruction.

Patients with CF suffer from a variety of medical complications, including severe pulmonary infections and gastrointestinal disorders that account for the increased morbidity and mortality associated with the disease (9). Meconium ileus commonly affects 10 to 20% of newborn human infants with CF and is caused by inspissated intestinal contents that cause obstruction or perforation of the bowel in utero or postnatally. It is encouraging that the lethal phenotype associated with the lack of the *CFTR* gene in the small intestine can be fully corrected by transfer of the h*CFTR* cDNA in a tissue-selective manner and that correction can be achieved even though the pattern of FABP promoter–driven expression differs from that of endogenous *CFTR*. These results provide further support for efforts to treat CF by gene therapy. The FABP-h$CFTR^{+/-}$–$CFTR^{-/-}$ bitransgenic mice will be useful in determining the abundance and distribution of *CFTR* expression that are required to correct the physiological and histologic abnormalities in the intestine of the CF mouse and will provide a more robust model to assess the effects of the null CF mutation on the respiratory tract.

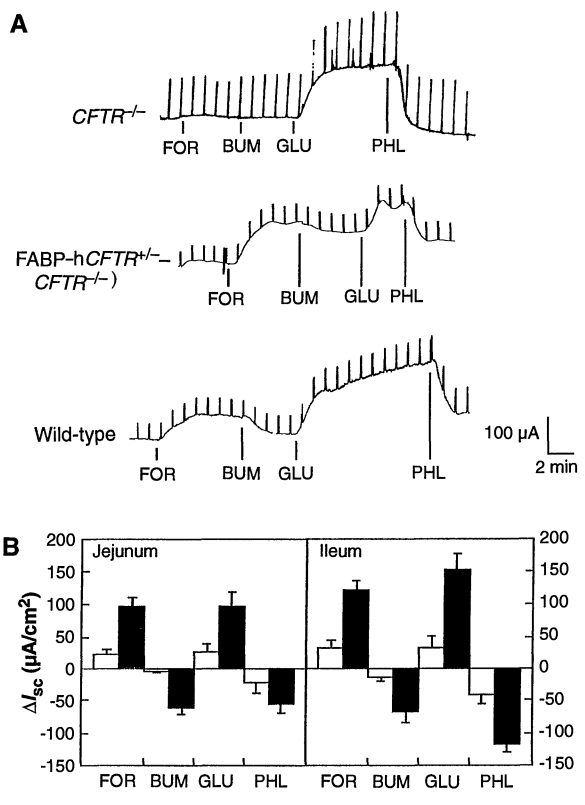

Fig. 4. (**A**) The I_{sc} recordings from ileal tissues. Sequential additions of 5 μM forskolin (FOR, both solutions), 100 μM bumetanide (BUM, serosal), 5 mM glucose (GLU, mucosal), and 200 μM phlorizin (PHL, mucosal) were as shown. (**B**) Mean ΔI_{sc} responses from jejunal and ileal tissues from FABP-h$CFTR^{+/-}$–$CFTR^{-/-}$ (n = 3; open bars) and wild-type (n = 5; solid bars) mice (*11*). The bars represent the mean ± SE of three to five tissue segments per mouse. The ΔI_{sc} represents the maximal response to addition of forskolin, bumetanide, glucose, and phlorizin.

REFERENCES AND NOTES

1. J. N. Snouwaert *et al.*, *Science* **257**, 1083 (1992).
2. S. M. Cohn, T. C. Simon, K. A. Roth, E. G. Birkenmeier, J. I. Gordon, *J. Cell Biol.* **119**, 27 (1992).
3. A 1206–base pair (bp) portion of the 5′ region of the gene encoding rat FABP, nucleotides −1178 to +28, was subcloned into pUC18, which contained a t intron polyadenylate cassette. A Sal I fragment containing nucleotides 122 to 4622 of the h*CFTR* cDNA sequence was placed 3′ to the FABP transcriptional element. The h*CFTR* cDNA fragment contained a silent T to C mutation at position 936 to stabilize the cDNA in high copy number plasmids by inactivating the cryptic bacterial promoter.
4. A chimeric FABP-h*CFTR* gene construct was microinjected into fertilized oocytes, producing transgenic mice from both heterozygotic $CFTR^{+/-}$ and wild-type FVB/N mice. The FABP-h*CFTR* transgene was detected by Southern blot analysis in founder mice and their offspring, with the use of a 4.5-kb h*CFTR* cDNA fragment as a probe, and the integrity of the DNA was confirmed by restriction fragment analysis. The copy number varied from 4 to 84 among nine distinct founder lines produced. Wild-type and heterozygotic $CFTR^{+/-}$ mice were identified by PCR (*1*) and were bred to establish permanent wild-type and $CFTR^{-/-}$ mouse lines bearing the FABP-h*CFTR* transgene.
5. Matings of mice from line A2 that were from FABP-h$CFTR^{+/-}$–$CFTR^{+/-}$ produced 101 offspring, of which 29 were homozygous $CFTR^{-/-}$ and bore the FABP-h*CFTR* transgene. Eight FABP-h$CFTR^{+/-}$–$CFTR^{-/-}$ mice were killed for study (at age 1 to 3 months) and were found to have been well. None had developed intestinal obstruction at ages ranging from 1.5 to 7.5 months. All FABP-h$CFTR^{+/-}$–$CFTR^{-/-}$ mice from line E9 (9 of 22 total offspring) were well at ages ranging from 1 to 4.5 months. FABP-h$CFTR^{+/-}$–$CFTR^{-/-}$ mice from l25 were not fully corrected; one died at 8.5 months from colonic obstruction, and others died at 1 to 2 months of age. Lines derived from A2, E9, and l25 bred well. Both male and female FABP-h$CFTR^{+/-}$–$CFTR^{-/-}$ mice from lines A2 and E9 were fertile.
6. A. E. O. Trezise and M. Buchwald, *Nature* **353**, 434 (1991); T. V. Strong, K. Boehm, F. S. Collins, *J. Clin. Invest.* **93**, 347 (1994).
7. L. L. Clark *et al.*, *Science* **257**, 1125 (1992).
8. M. J. Welsh, P. L. Smith, R. A. Frizzell, *ibid.* **218**, 1219 (1982); C. Siemer and H. Gogelein, *Pflueg. Arch. Eur. J. Physiol.* **424**, 321 (1993).
9. T. F. Boat, M. J. Welsh, A. L. Beaudet, *The Metabolic Basis of Inherited Disease* (McGraw-Hill, New York, 1989), pp. 2649–2680.
10. J. A. Whitsett *et al.*, *Nature Genet.* **2**, 13 (1992).
11. Tissue segments 5 mm in length were mounted on plastic adaptor rings and inserted into modified Ussing chambers with an exposed area of 0.1 cm^2. The standard bathing solution (37°C) contained 116 mM NaCl, 1.2 mM $MgCl_2$, 25 mM $NaHCO_3$, 1.2 mM $NaHPO_4$, 10 mM mannitol (mucosal), and 10 mM glucose (serosal) (pH 7.4). The I_{sc} was monitored continuously; the transepithelial conductance was determined periodically by measuring the current needed to clamp the transepithelial potential to +1 mV (+2 mV for the $CFTR^{-/-}$ I_{sc} trace in Fig. 4A). Adjacent jejunal segments were taken from the middle portion of the small intestine. Adjacent ileal segments were taken from the distal small intestine immediately proximal to the ileocecal juncture.

12. We thank X.-Y. Hu for technical assistance and B. Koller for providing $CFTR^{-/-}$ mice. Supported by the Cystic Fibrosis Foundation and by grants from NIH [HL51832 (from the Center for Gene Therapy for Cystic Fibrosis), DK38518, and HL49004].

21 June 1994; accepted 30 September 1994